Beamspace Channel Estimation for Wideband Millimeter-Wave MIMO with Lens Antenna Array

Xinyu Gao*, Linglong Dai*, Shidong Zhou*, Akbar M. Sayeed†, and Lajos Hanzo‡
*Tsinghua National Laboratory for Information Science and Technology, Tsinghua University, Beijing 100084, China
†Electrical and Computer Engineering, University of Wisconsin-Madison, WI 53706, USA
‡Electronics and Computer Science, University of Southampton, Southampton SO17 1BJ, U.K.

***Abstract*—Beamspace channel estimation is essential for wideband millimeter-wave (mmWave) MIMO with lens antenna array to achieve the substantial increase in data rates, but with a considerably reduced number of radio-frequency chains. However, most of existing beamspace channel estimation schemes are designed for narrowband mmWave systems, while a very few wideband schemes assume that the beamspace channel enjoys the ideal common support in frequency domain. In this paper, inspired by the classical successive interference cancellation for multi-user detection, we propose an efficient successive support detection (SSD) based beamspace channel estimation scheme without the assumption of common support. Specifically, we first demonstrate that each path component of the wideband beamspace channel exhibits a unique frequency-varying sparse structure. Based on this, we then estimate all sparse path components one by one. For each path component, its supports at different frequencies are jointly estimated to improve the estimation accuracy, and then its influence is removed to estimate the remained path components. Once all path components have been estimated, the wideband beamspace channel can be recovered at a low complexity. Simulation results verify that the proposed SSD based beamspace channel estimation scheme is able to achieve higher accuracy than existing wideband schemes.**

I. Introduction

Millimeter-wave (mmWave) multiple-input multiple-output (MIMO) with lens antenna array is a promising technique for 5G wireless communications [1]. On one hand, it can significantly improve the data rates due to the larger bandwidth (2-5 GHz) [2]. On the other hand, by employing lens antenna array, it can focus the mmWave signals from different directions on different antennas, and thus transform the spatial channel to its sparse beamspace representation (beamspace channel) [3]. This enables us to select only a small number of power-focusing beams to significantly reduce the MIMO dimension. Consequently, the number of radio-frequency (RF) chains can be saved, and the high energy consumption and hardware cost in mmWave MIMO systems can be relieved [4].

To select the power-focusing beams, the high-dimensional wideband beamspace channel is required at the base station (BS), but this imposes quite a challenge, since the number of RF chains is much lower than the number of antennas [5]. To overcome this challenge, some beamspace channel estimation schemes have been proposed recently. For example, a beam training-based scheme was proposed in [6]. It first trained all the beams to search the ones with strong power and reduce the channel dimension. Then, the least squares (LS) algorithm was employed to estimate the dimension-reduced beamspace channel. In [7], a support detection based scheme was proposed, which directly estimated the sparse beamspace channel at a reduced pilot overhead. However, these schemes are designed for narrowband mmWave systems, while mmWave systems are more likely to be wideband to achieve high data rates. For wideband mmWave systems, there are only a few recent works. Specifically, a simultaneous orthogonal matching pursuit (SOMP) based scheme was proposed in [8], which assumed that the wideband beamspace channels had the same support at different frequencies (i.e., common support). In addition, an OMP based scheme was proposed in [9]. It first estimated the supports of the wideband beamspace channel at some frequencies independently by the OMP algorithm. Then, it combined the supports to create a common support at all frequencies. Nevertheless, the assumption of common support in [8], [9] is not really valid in practice, as the supports of wideband beamspace channel tend to be frequency-dependent when the bandwidth and the number of antennas are large, which is called as beam squint in the literature [10].

In this paper, inspired by the classical successive interference cancellation (SIC) for multi-user detection [11], we propose a successive support detection (SSD) based beamspace channel estimation scheme without the ideal assumption of common support. Specifically, we first demonstrate that each path component of the wideband beamspace channel exhibits a unique frequency-varying sparse structure, i.e., its frequency-dependent supports can be determined by its spatial direction at the carrier frequency. We further show that this spatial direction can be estimated by tentatively generating several beamspace windows (BWins) to capture the path power. Based on these, we then propose to decompose the original complete wideband beamspace channel estimation problem into a series of sub-problems, each of which only considers one path component. For each path component, its supports at different frequencies are jointly estimated to improve the estimation accuracy, and then its influence is removed to estimate the remained path components following the similar idea of SIC. Simulation results verify that the proposed scheme enjoys lower complexity and higher accuracy than existing schemes.

Notation: Lower-case and upper-case boldface letters $\mathbf{a}$ and $\mathbf{A}$ denote a vector and a matrix, respectively; $\mathbf{A}^T$, $\mathbf{A}^H$, $\mathbf{A}^{-1}$, and $\mathbf{A}^\dagger$ denote the transpose, conjugate transpose, inverse, and pseudo inverse of matrix $\mathbf{A}$, respectively; $\|\mathbf{A}\|_F$ denotes the Frobenius norm of matrix $\mathbf{A}$; $|a|$ denotes the amplitude of

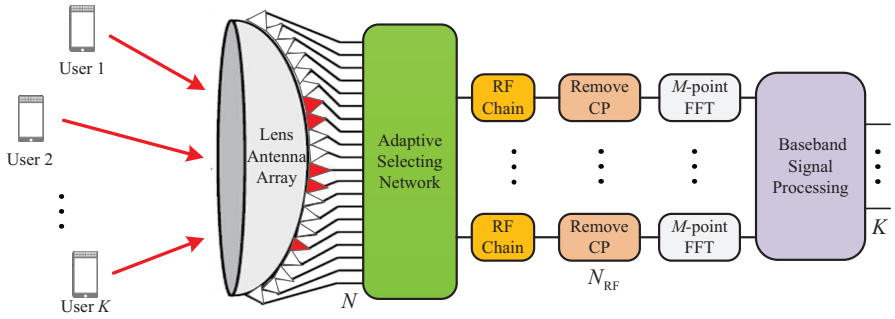

Fig. 1. System architecture of wideband mmWave MIMO-OFDM system with lens antenna array.

scalar a; $\mathrm{Card}(\mathcal{A})$ denotes the cardinality of set $\mathcal{A}$; Finally, $\mathbf{I}_N$ is the identity matrix of size $N \times N$.

II. System Model

As shown in Fig. 1, we consider a uplink time division duplexing (TDD) based wideband mmWave MIMO-OFDM system with M sub-carriers. The BS employs an N-element lens antenna array and N_{RF} RF chains to simultaneously serve K single-antenna users [10]. In this section, we will first introduce the wideband beamspace channel, and then formulate the wideband beamspace channel estimation problem.

A. Wideband beamspace channel

We commence with the conventional mmWave MIMO channel in the spatial domain. The widely used Saleh-Valenzuela multipath channel model [12] is adopted, where the $N \times 1$ spatial channel $\mathbf{h}_m$ of a certain user at sub-carrier m ($m = 1, 2, \cdots, M$) can be presented as

$$\mathbf{h}_m = \sqrt{\frac{N}{L}} \sum_{l=1}^{L} \beta_l e^{-j2\pi\tau_l f_m} \mathbf{a}(\varphi_{l,m}), \tag{1}$$

where L is the number of resolvable paths, β_l and τ_l are the complex gain and time delay of the lth path, respectively, $\varphi_{l,m}$ is the spatial direction at sub-carrier m defined as

$$\varphi_{l,m} = \frac{f_m}{c} d \sin\theta_l, \tag{2}$$

where $f_m = f_c + \frac{f_s}{M}\left(m - 1 - \frac{M-1}{2}\right)$ is the frequency at sub-carrier m with f_c and f_s presenting the carrier frequency and bandwidth (sampling rate), respectively, c is the light speed, θ_l is the physical direction, and d is the antenna spacing which is usually designed according to the carrier frequency as $d = c/2f_c$ [12]. Note that in narrowband mmWave systems, $f_m \approx f_c$, and $\varphi_{l,m} \approx \frac{1}{2}\sin\theta_l$ is frequency-independent. However, in wideband mmWave systems, $f_m \neq f_c$, and $\varphi_{l,m}$ is frequency-dependent. Finally, $\mathbf{a}(\varphi_{l,m})$ is the array response vector of $\varphi_{l,m}$. For the typical N-element uniform linear array (ULA), we have $\mathbf{a}(\varphi_{l,m}) = \frac{1}{\sqrt{N}} e^{-j2\pi\varphi_{l,m}\mathbf{p}}$, where $\mathbf{p} = \left[-\frac{N-1}{2}, -\frac{N-3}{2}, \cdots, \frac{N-1}{2}\right]^T$ [4].

The spatial channel $\mathbf{h}_m$ can be transformed to its beamspace representation by the lens antenna array, as shown in Fig. 1. Essentially, the lens antenna array plays the role of the spatial discrete fourier transform (DFT) matrix $\mathbf{U}$ of size $N \times N$, which contains N orthogonal array response vectors of N directions (beams) covering the entire spatial space as

$$\mathbf{U} = \left[\mathbf{a}(\bar{\varphi}_1), \mathbf{a}(\bar{\varphi}_2), \cdots, \mathbf{a}(\bar{\varphi}_N)\right]^H, \tag{3}$$

where $\bar{\varphi}_n = \frac{1}{N}\left(n - \frac{N+1}{2}\right)$ for $n = 1, 2, \cdots, N$ are the spatial directions predefined by the lens antenna array. Accordingly, the wideband beamspace channel $\tilde{\mathbf{h}}_m$ can be presented by

$$\tilde{\mathbf{h}}_m = \mathbf{U}\mathbf{h}_m = \sqrt{\frac{N}{L}} \sum_{l=1}^{L} \beta_l e^{-j2\pi\tau_l f_m} \tilde{\mathbf{c}}_{l,m}, \tag{4}$$

where $\tilde{\mathbf{c}}_{l,m}$ denotes the lth path component at sub-carrier m in the beamspace. Particularly, $\tilde{\mathbf{c}}_{l,m}$ is determined by $\varphi_{l,m}$ as

$$\begin{aligned} \tilde{\mathbf{c}}_{l,m} &= \mathbf{U}\mathbf{a}(\varphi_{l,m}) \\ &= \left[\Xi(\varphi_{l,m} - \bar{\varphi}_1), \Xi(\varphi_{l,m} - \bar{\varphi}_2), \cdots, \Xi(\varphi_{l,m} - \bar{\varphi}_N)\right]^T, \end{aligned} \tag{5}$$

where $\Xi(x) = \frac{\sin N\pi x}{\sin \pi x}$ is the Dirichlet sinc function [4]. Based on the power-focusing property of $\Xi(x)$ [4], [7], we know that the most power of $\tilde{\mathbf{c}}_{l,m}$ is focused on only a small number of elements. In addition, due to the limited scattering in mmWave systems, L is usually small (e.g., $L = 3$ [13]). As a result, the wideband beamspace channel $\tilde{\mathbf{h}}_m$ in (4) is a sparse (compressive) vector. However, since $\varphi_{l,m}$ in (2) is frequency-dependent in wideband mmWave systems, the support of $\tilde{\mathbf{h}}_m$ should be different at different sub-carriers. This effect is called as beam squint [10][1], which has not been considered in the existing beamspace channel estimation schemes [8], [9].

B. Problem formulation

In TDD systems, users need to transmit the pilot sequences to the BS for uplink channel estimation. In this paper, we adopt the widely used orthogonal pilot transmission strategy [14], where the channel estimation invoked for each user is independent. Consider a certain user without loss of generality, and define $s_{m,q}$ as its pilot at sub-carrier m in instant q (each user transmits one pilot in one instant) before M-point IFFT and cyclic prefix (CP) adding [9]. Then, as shown in Fig. 1, the $N_{\mathrm{RF}} \times 1$ received pilot vector $\mathbf{y}_{m,q}$ in the baseband at BS after combining (realized by the adaptive selecting network [7]), CP removal, and M-point FFT [9] can be presented as

$$\mathbf{y}_{m,q} = \mathbf{W}_q \tilde{\mathbf{h}}_m s_{m,q} + \mathbf{W}_q \mathbf{n}_{m,q}, \quad m = 1, 2, \cdots, M, \tag{6}$$

[1]Note that the effect of beam squint will be more pronounced in wideband mmWave MIMO with conventional phased array [12], and the proposed scheme can be also used in this case.

where $\mathbf{W}_q$ of size $N_{\mathrm{RF}} \times N$ is the combining matrix (it is fixed at different sub-carriers due to the analog hardware limitation [9]) and $\mathbf{n}_{m,q} \sim \mathcal{CN}\left(0, \sigma^2 \mathbf{I}_N\right)$ of size $N \times 1$ is noise vector with σ^2 presenting the noise power. After Q instants of pilot transmission, we can obtain the overall measurement vector $\bar{\mathbf{y}}_m = \left[\mathbf{y}_{m,1}^T, \mathbf{y}_{m,2}^T, \cdots, \mathbf{y}_{m,Q}^T\right]^T$ as

$$\bar{\mathbf{y}}_m = \bar{\mathbf{W}} \tilde{\mathbf{h}}_m + \mathbf{n}_m^{\mathrm{eff}}, \quad m = 1, 2, \cdots, M, \tag{7}$$

where we assume $s_{m,q} = 1$ for $q = 1, 2, \cdots, Q$ without loss of generality, $\bar{\mathbf{W}} = \left[\mathbf{W}_1^T, \mathbf{W}_2^T, \cdots, \mathbf{W}_Q^T\right]^T$ of size $QN_{\mathrm{RF}} \times N$ is the overall combing matrix, whose elements can be randomly selected from the set $\frac{1}{\sqrt{QN_{\mathrm{RF}}}}\{-1, +1\}$ with equal probability if they are realized by the low-cost 1-bit phase shifters [7]. Finally, $\mathbf{n}_m^{\mathrm{eff}}$ is the effective noise vector.

The target of beamspace channel estimation is to recover $\tilde{\mathbf{h}}_m$ given $\bar{\mathbf{y}}_m$ and $\bar{\mathbf{W}}$ in (7). Since $\tilde{\mathbf{h}}_m$ is sparse, this problem can be solved based on compressive sensing (CS) with significantly reduced number of instants (i.e., $Q \ll (N/N_{\mathrm{RF}})$) [15]. However, most of existing schemes based on CS are designed for narrowband mmWave systems [6], [16], while mmWave systems tend to be wideband to achieve high data rates. In fact, only the schemes in [8], [9] have been designed for wideband mmWave systems. However, both of them assume the ideal common support, which may suffer from accuracy degradation in practice due to the beam squint [10].

III. Wideband Beamspace Channel Estimation

In this section, we will first demonstrate the sparse structure of wideband beamspace channel. Based on this sparse structure, we then propose an efficient SSD based scheme. Finally, the complexity analysis of the proposed scheme is provided.

A. Sparse structure of wideband beamspace channel

Due to beam squint, the assumption of common support does not hold. However, the wideband beamspace channel still enjoys a sparse structure as proved by the following lemmas.

Lemma 1. *Consider the lth path component of the wideband beamspace channel. The frequency-varying path supports $\mathcal{T}_{l,m}$ of $\tilde{\mathbf{c}}_{l,m}$ in (4) for $m = 1, 2, \cdots, M$ can be determined by the spatial direction $\varphi_{l,c}$ of the lth path at the carrier frequency f_c, which is defined as $\varphi_{l,c} = (f_c/c)\, d \sin\theta_l = (1/2)\sin\theta_l$.*

Proof: Based on the analysis in [7], the strongest element index $n_{l,m}^{\star}$ of $\tilde{\mathbf{c}}_{l,m}$ can be calculated based on $\varphi_{l,m}$ as

$$n_{l,m}^{\star} = \arg\min_n \left|\varphi_{l,m} - \bar{\varphi}_n\right|, \tag{8}$$

and the support of $\tilde{\mathbf{c}}_{l,m}$ can be obtained by

$$\mathcal{T}_{l,m} = \Theta_N\left\{n_{l,m}^{\star} - \Omega, \cdots n_{l,m}^{\star} + \Omega\right\}, \tag{9}$$

where $\Theta_N(x) = \mathrm{mod}_N(x-1) + 1$ is the mod function guaranteeing that all elements in $\mathcal{T}_{l,m}$ belong to $\{1, 2, \cdots, N\}$, and Ω determines how much power can be preserved by assuming $\tilde{\mathbf{c}}_{l,m}$ as a sparse vector with support $\mathcal{T}_{l,m}$. For example, when $N = 256$ and $\Omega = 4$, more than 96% of the power can be preserved [7].

On the other hand, based on the definition of $\varphi_{l,c}$, $\varphi_{l,m}$ in (2) can be rewritten following [10] as

$$\varphi_{l,m} = \left\{1 + \frac{f_s}{M f_c}\left(m - 1 - \frac{M-1}{2}\right)\right\}\varphi_{l,c}, \tag{10}$$

which can be determined by $\varphi_{l,c}$. As a result, once $\varphi_{l,c}$ is known, the path supports $\mathcal{T}_{l,m}$ for $m = 1, 2, \cdots, M$ can be directly obtained based on (8) and (9). ■

Lemma 1 implies that $\varphi_{l,c}$ is a crucial parameter to determine $\mathcal{T}_{l,m}$ for $m = 1, 2, \cdots, M$. In the following **Lemma 2**, we will give some insights about how to estimate $\varphi_{l,c}$.

Lemma 2. *Define $\mathbf{C}_n = [\tilde{\mathbf{c}}_{l,1}, \tilde{\mathbf{c}}_{l,2}, \cdots, \tilde{\mathbf{c}}_{l,M}]$ by assuming $\varphi_{l,c} = \bar{\varphi}_n$. Let $\Upsilon_n = \Theta_N\{n - \Delta_n, \cdots n + \Delta_n\}$ be a BWin centred around n. Then, the ratio γ between the power of the sub-matrix $\mathbf{C}_n(\Upsilon_n, :)$ (extracting the rows indexed by Υ_n of $\mathbf{C}_n$) and the power of $\mathbf{C}_n$ can be presented as*

$$\gamma = \frac{f_c}{f_s \varphi_{l,c}} \sum_{s=-\Delta_n}^{\Delta_n} \int_{-f_s\varphi_{l,c}/2f_c}^{f_s\varphi_{l,c}/2f_c} \Xi^2\left(\frac{s}{N} + \Delta\varphi\right) d\Delta\varphi. \tag{11}$$

Proof: Based on (5), γ can be calculated as

$$\gamma = \frac{\|\mathbf{C}_n(\Upsilon_n, :)\|_F^2}{\|\mathbf{C}_n\|_F^2} = \frac{1}{M}\sum_{s\in\Upsilon_n}\sum_{m=1}^{M}\Xi^2(\varphi_{l,m} - \bar{\varphi}_s), \tag{12}$$

where we have $\|\mathbf{C}_n\|_F^2 = \sum_{s=1}^{N}\sum_{m=1}^{M}\Xi^2(\varphi_{l,m} - \bar{\varphi}_s) = M$. Defining $\Delta\varphi_m = \frac{f_s\varphi_{l,c}}{Mf_c}\left(m - 1 - \frac{M-1}{2}\right)$, we can rewrite (12) based on (10) as

$$\begin{aligned}\gamma &= \frac{1}{M}\sum_{s\in\Upsilon_n}\sum_{m=1}^{M}\Xi^2(\varphi_{l,c} + \Delta\varphi_m - \bar{\varphi}_s) \\ &\overset{(a)}{=} \frac{1}{M}\sum_{s=-\Delta_n}^{\Delta_n}\sum_{m=1}^{M}\Xi^2\left(\frac{s}{N} + \Delta\varphi_m\right),\end{aligned} \tag{13}$$

where (a) is true due to the assumption $\varphi_{l,c} = \bar{\varphi}_n$. Note that M is usually a large number (e.g., $M = 128$). Therefore, the second summation in (13) can be written in its integral form

$$\frac{Mf_c}{f_s\varphi_{l,c}}\int_{-f_s\varphi_{l,c}/2f_c}^{f_s\varphi_{l,c}/2f_c}\Xi^2\left(\frac{s}{N} + \Delta\varphi\right)d\Delta\varphi, \tag{14}$$

where the integral interval is determined by $\Delta\varphi_1$ and $\Delta\varphi_M$. Based on (13) and (14), the conclusion (11) can be derived. ■

Lemma 2 implies that if $\varphi_{l,c} = \bar{\varphi}_n$, the most power of $\mathbf{C}_n$ is focused in a BWin Υ_n centered around n. For example, given $N = 256$, $f_c = 28$ GHz, $f_s = 4$ GHz, $\varphi_{l,c} = \bar{\varphi}_1$, we can capture the $\gamma \approx 92\%$ power of $\mathbf{C}_1$ by using the BWin $\Upsilon_1 = \Theta_{256}\{1 - 8, \cdots, 1 + 8\}$ ($\Delta_1 = 8$). On the other hand, if $\varphi_{l,c} \neq \bar{\varphi}_1$, e.g., $\varphi_{l,c} = \bar{\varphi}_{10}$, using this Υ_1 to capture the power of $\mathbf{C}_{10}$ will lead to serious power leakage, where we only have $\gamma \approx 47\%$. Such observation is further illustrated in Fig. 2 (a) and (b). This indicates that the BWin Υ_n centered around n can be considered as a feature specialized for $\bar{\varphi}_n$, which can be utilized to estimate $\bar{\varphi}_n$.

The next problem is how to design Δ_n in Υ_n. Generally speaking, when Δ_n is too large or too small, there may be

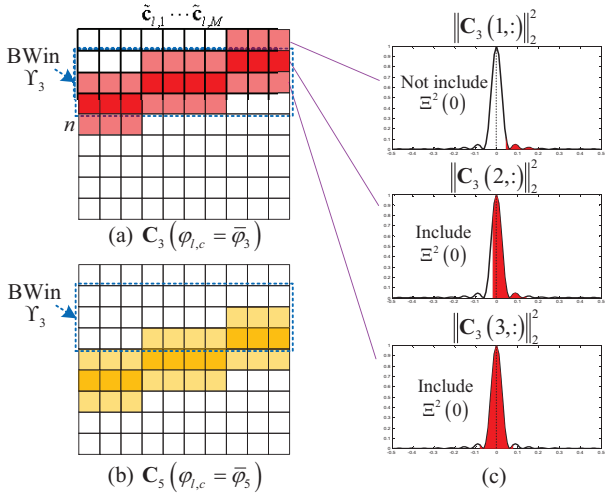

Fig. 2. Illustration of the power distribution: a) $\mathbf{C}_3$; b) $\mathbf{C}_5$; c) $\mathbf{C}_3(1,:)$, $\mathbf{C}_3(2,:)$, and $\mathbf{C}_3(3,:)$.

multiple BWins that capturing the similar power of $\mathbf{C}_n$. This makes the estimation of $\varphi_{l,c}$ sensitive to noise or interference in practice. Therefore, Δ_n should be carefully designed to make the power leakage incurred by $\varphi_{l,c}\neq\bar{\varphi}_n$ as serious as possible. On the other hand, we observe from Fig. 2 (c) that if the integral in (11) includes $\Xi^2(0)$, it will be a large value. Otherwise, it should be small. Based on these facts, the optimal Δ_n should be designed to satisfy: when we use Υ_n to capture the power of $\mathbf{C}_n$ with $\varphi_{l,c}=\bar{\varphi}_n$, it includes $\Xi^2(0)$, while when we use Υ_n to capture the power of $\mathbf{C}_{n'}$ with $\varphi_{l,c}=\bar{\varphi}_{n'}\neq\bar{\varphi}_n$, it does not. This indicates that

$$\left\lfloor\frac{\Delta_n}{N}-\frac{f_s\left|\bar{\varphi}_n\right|}{2f_c}\right\rfloor=0\Rightarrow\Delta_n=\left\lfloor\frac{Nf_s\left|\bar{\varphi}_n\right|}{2f_c}\right\rfloor, \tag{15}$$

where $\lfloor x\rfloor$ returns the largest integer smaller than x. Note that this value has the similar form to the channel spread factor defined in [10], but they are actually two different parameters designed for different purposes and derived in different ways.

B. SSD based beamspace channel estimation scheme

Based on the discussions above, we propose an efficient SSD based beamspace channel estimation scheme. Its key idea is to decompose the total channel estimation problem into a series of sub-problems, and each one only considers one path component. We first estimate the supports of the strongest path component at all sub-carriers jointly. Then, its influence is removed for the remaining estimation. Such procedure is repeated until all path components are estimated[2]. To realize these, we first rewrite (7) as

$$\bar{\mathbf{Y}}=\bar{\mathbf{W}}\tilde{\mathbf{H}}+\mathbf{N}, \tag{16}$$

where $\bar{\mathbf{Y}}=[\bar{\mathbf{y}}_1,\bar{\mathbf{y}}_2,\cdots,\bar{\mathbf{y}}_M]$, $\tilde{\mathbf{H}}=\left[\tilde{\mathbf{h}}_1,\tilde{\mathbf{h}}_2,\cdots,\tilde{\mathbf{h}}_M\right]$, and $\mathbf{N}=\left[\mathbf{n}_1^{\text{eff}},\mathbf{n}_2^{\text{eff}},\cdots,\mathbf{n}_M^{\text{eff}}\right]$. Then, the pseudo-code of the proposed SSD based scheme is summarized in **Algorithm 1**.

For the initialization, we set $\mathbf{R}=[\mathbf{r}_1,\mathbf{r}_2\cdots,\mathbf{r}_M]=\bar{\mathbf{Y}}$, where $\mathbf{r}_m$ denotes the residual at sub-carrier m.

[2]In practice, the number of resolvable paths L can be usually obtained in advance by channel measurement [13].

Input:
Measurement matrix: $\bar{\mathbf{Y}}$
Combining matrix: $\bar{\mathbf{W}}$
Total number of channel paths: L
Initialization: $\mathbf{R}=\bar{\mathbf{Y}}$
for $1\leq l\leq L$
1. $\Upsilon_n=\Theta_N\{n-\Delta_n,\cdots,n+\Delta_n\}$, $\Delta_n=\left\lfloor\frac{Nf_s|\bar{\varphi}_n|}{2f_c}\right\rfloor$
2. $\mathbf{A}_l=\bar{\mathbf{W}}^H\mathbf{R}$
3. $n_{l,c}^\star=\arg\max_n\frac{\|\mathbf{A}_l(\Upsilon_n,:)\|_F^2}{\text{Card}(\Upsilon_n)}$
4. $\varphi_{l,c}=\bar{\varphi}_{n_{l,c}^\star}$
   for $1\leq m\leq M$
5. $\varphi_{l,m}=\left\{1+\frac{f_s}{Mf_c}\left(m-1-\frac{M-1}{2}\right)\right\}\varphi_{l,c}$
6. $n_{l,m}^\star=\arg\min_n|\varphi_{l,m}-\bar{\varphi}_n|$
7. $\mathcal{T}_{l,m}=\Theta_N\left\{n_{l,m}^\star-\Omega,\cdots n_{l,m}^\star+\Omega\right\}$
   for $1\leq i\leq I$
8. $\tilde{\mathbf{c}}_{l,m}=\mathbf{0}_{N\times1}$, $\tilde{\mathbf{c}}_{l,m}(\mathcal{T}_{l,m})=\bar{\mathbf{W}}^\dagger(:,\mathcal{T}_{l,m})\mathbf{r}_m$
9. $n_{l,m}^\star=\arg\max_n|\tilde{\mathbf{c}}_{l,m}(n)|$
10. $\mathcal{T}_{l,m}=\Theta_N\left\{n_{l,m}^\star-\Omega,\cdots n_{l,m}^\star+\Omega\right\}$
    end for
11. $\tilde{\mathbf{c}}_{l,m}=\mathbf{0}_{N\times1}$, $\tilde{\mathbf{c}}_{l,m}(\mathcal{T}_{l,m})=\bar{\mathbf{W}}^\dagger(:,\mathcal{T}_{l,m})\mathbf{r}_m$
12. $\mathbf{r}_m=\mathbf{r}_m-\bar{\mathbf{W}}(:,\mathcal{T}_{l,m})\tilde{\mathbf{c}}_{l,m}(\mathcal{T}_{l,m})$
    end for
end for
for $1\leq m\leq M$
13. $\tilde{\mathcal{T}}_m=\mathcal{T}_{1,m}\cup\mathcal{T}_{2,m}\cup\cdots\cup\mathcal{T}_{L,m}$
14. $\tilde{\mathbf{h}}_m=\mathbf{0}_{N\times1}$, $\tilde{\mathbf{h}}_m\left(\tilde{\mathcal{T}}_m\right)=\bar{\mathbf{W}}^\dagger\left(:,\tilde{\mathcal{T}}_m\right)\bar{\mathbf{y}}_m$
end for
Output:
Estimated beamspace channel: $\tilde{\mathbf{H}}=\left[\tilde{\mathbf{h}}_1,\tilde{\mathbf{h}}_2,\cdots,\tilde{\mathbf{h}}_M\right]$

Algorithm 1: SSD based beamspace channel estimation.

For the l-th path component, we first estimate $\varphi_{l,c}$ based on **Lemma 2**. Specifically, in step 1, we generate N BWins $\Upsilon_n=\Theta_N\{n-\Delta_n,\cdots,n+\Delta_n\}$ with $\Delta_n=\left\lfloor\frac{Nf_s|\bar{\varphi}_n|}{2f_c}\right\rfloor$ for $n=1,2,\cdots,N$ according to (15). Then, in step 2, we calculate the correlation matrix $\mathbf{A}_l$ between $\bar{\mathbf{W}}$ and $\mathbf{R}$ as $\mathbf{A}_l=\bar{\mathbf{W}}^H\mathbf{R}$ following the similar idea in the OMP or SOMP algorithms [15]. In step 3, we can utilize the N BWins to capture the power of $\mathbf{A}_l$, and obtain the spatial direction index $n_{l,c}^\star$ of the l-th path component at the carrier frequency as

$$n_{l,c}^\star=\arg\max_n\frac{\|\mathbf{A}_l(\Upsilon_n,:)\|_F^2}{\text{Card}(\Upsilon_n)}, \tag{17}$$

where we divide $\|\mathbf{A}_l(\Upsilon_n,:)\|_F^2$ by $\text{Card}(\Upsilon_n)=2\Delta_n+1$ to avoid that larger BWin captures more noise power. Finally, in step 4, $\varphi_{l,c}$ is estimated as $\varphi_{l,c}=\bar{\varphi}_{n_{l,c}^\star}$.

After $\varphi_{l,c}$ has been estimated, the frequency-varying path supports $\mathcal{T}_{l,m}$ for $m=1,2,\cdots,M$ can be obtained according to **Lemma 1**. Specifically, in steps 5 and 6, we compute the spatial direction $\varphi_{l,m}$ and the strongest element index $n_{l,m}^\star$ of the lth path component at sub-carrier m based on (10) and (8), respectively. Then, in step 7, we can obtain the path

support $\mathcal{T}_{l,m}$ based on (9). It is worth pointing out that in practice, due to the noise and the column correlation of $\bar{\mathbf{W}}$ (i.e., $\bar{\mathbf{W}}^H\bar{\mathbf{W}} \neq \mathbf{I}_N$ since $QN_{\mathrm{RF}} \ll N$), the estimation of $\varphi_{l,c}$ may be inaccurate, which makes the estimated $\mathcal{T}_{l,m}$ different from the actual one. To overcome this problem, we propose to take $\mathcal{T}_{l,m}$ in step 7 as the initial solution, and estimate the nonzero elements of the lth path component $\tilde{\mathbf{c}}_{l,m}$ in step 8 as

$$\tilde{\mathbf{c}}_{l,m}\left(\mathcal{T}_{l,m}\right) = \bar{\mathbf{W}}^{\dagger}\left(:,\mathcal{T}_{l,m}\right)\mathbf{r}_m, \tag{18}$$

where $\tilde{\mathbf{c}}_{l,m}\left(\mathcal{T}_{l,m}\right)$ is the sub-vector of $\tilde{\mathbf{c}}_{l,m}$ indexed by $\mathcal{T}_{l,m}$. Then, $n_{l,m}^{\star}$ is re-computed as $n_{l,m}^{\star} = \arg\max_n |\tilde{\mathbf{c}}_{l,m}(n)|$ in step 9, and $\mathcal{T}_{l,m}$ is re-estimated in step 10. Steps 8-10 can be repeated for I times to progressively refine $\mathcal{T}_{l,m}$.

After the support estimation, we remove the influence of the lth path component to estimate the remained path components. Specifically, in step 11, based on $\mathcal{T}_{l,m}$, we estimate the nonzero elements of the lth path component $\tilde{\mathbf{c}}_{l,m}$ at sub-carrier m by LS algorithm as in (18). Then, its influence is removed by $\mathbf{r}_m = \mathbf{r}_m - \bar{\mathbf{W}}\left(:,\mathcal{T}_{l,m}\right)\tilde{\mathbf{c}}_{l,m}\left(\mathcal{T}_{l,m}\right)$ in step 12.

Such procedure above will be repeated until the path supports of all path components are estimated. In the end, we estimate $\tilde{\mathbf{h}}_1, \tilde{\mathbf{h}}_2, \cdots, \tilde{\mathbf{h}}_M$ independently. Specifically, in step 13, we formulate the complete support $\tilde{\mathcal{T}}_m$ of $\tilde{\mathbf{h}}_m$ as

$$\tilde{\mathcal{T}}_m = \mathcal{T}_{1,m} \cup \mathcal{T}_{2,m} \cup \cdots \cup \mathcal{T}_{L,m}. \tag{19}$$

Then, in the step 14, the nonzero elements of $\tilde{\mathbf{h}}_m$ are estimated by the LS algorithm as $\tilde{\mathbf{h}}_m\left(\tilde{\mathcal{T}}_m\right) = \bar{\mathbf{W}}^{\dagger}\left(:,\tilde{\mathcal{T}}_m\right)\bar{\mathbf{y}}_m$.

The key difference between our scheme and conventional schemes is the support detection. For example, for OMP based scheme [9], the supports of wideband beamspace channel at different sub-carriers are estimated independently, which are vulnerable to noise. As a result, the detected supports may be inaccurate, especially in the low SNR region [15]. For SOMP based scheme [8], the support at different sub-carriers are estimated jointly, but it assumes common support. Due to the beam squint, this assumption will lead to serious performance loss, especially in the high SNR region. By contrast, the proposed scheme recovers the supports jointly without the assumption of common support. By fully exploiting the frequency-varying sparse structure of wideband beamspace channel, our scheme can achieve much higher accuracy. These conclusions will be further verified in Section IV.

Finally, we would like to point out that the proposed scheme can be extended to the case with multiple-antenna users. In this case, the beamspace channel in (4) should be a sparse matrix with 2D sparse structure similar to the one proved in Section III-A. Therefore, we can first vectorize the sparse matrix as in [9]. Then, **Algorithm 1** can be also extended to estimate the wideband beamspace channel.

C. Complexity analysis

In this subsection, we evaluate the complexity of the proposed SSD-based scheme in terms of the number of complex multiplications. According to **Algorithm 1**, we observe that the complexity is dominated by steps 2, 3, 8, 11, 12, 14.

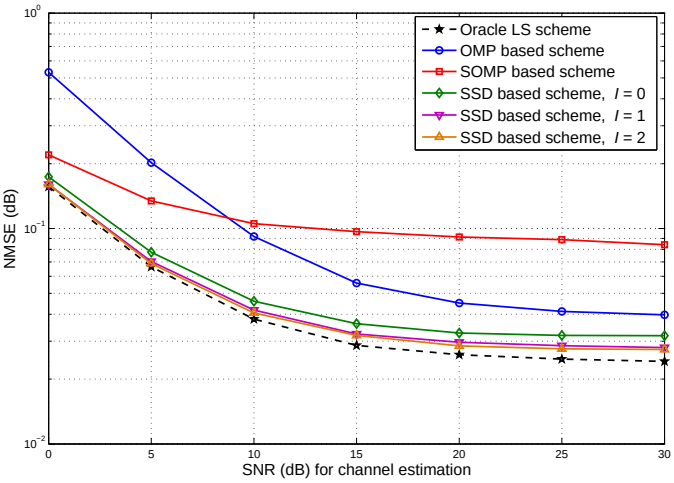

Fig. 3. NMSE comparison against the SNR for channel estimation.

In step 2, we need to compute the multiplication between $\bar{\mathbf{W}}^H$ of size $N \times QN_{\mathrm{RF}}$ and $\mathbf{R}$ of size $QN_{\mathrm{RF}} \times M$, which has the complexity in order of $\mathcal{O}\left(NN_{\mathrm{RF}}MQ\right)$. In step 3, the power of N sub-matrices $\mathbf{A}_l\left(\Upsilon_n,:\right)$ for $n = 1, 2, \cdots, N$ is calculated. This can be solved by calculating the power of N rows of $\mathbf{A}_l$ in advance, where the complexity is $\mathcal{O}\left(NM\right)$. In steps 8 and 11, the pseudo inverse of $\bar{\mathbf{W}}\left(:,\mathcal{T}_{l,m}\right)$ of size $QN_{\mathrm{RF}} \times (2\Omega+1)$, and the multiplication between $\bar{\mathbf{W}}^{\dagger}\left(:,\mathcal{T}_{l,m}\right)$ of size $(2\Omega+1) \times QN_{\mathrm{RF}}$ and $\mathbf{r}_m$ of size $QN_{\mathrm{RF}} \times 1$ are required. Therefore, both of these two steps involve the complexity $\mathcal{O}\left(N_{\mathrm{RF}}Q\Omega^2\right)$. In step 12, we compute the multiplication between $\bar{\mathbf{W}}\left(:,\mathcal{T}_{l,m}\right)$ and $\tilde{\mathbf{c}}_{l,m}\left(\mathcal{T}_{l,m}\right)$ of size $(2\Omega+1) \times 1$ with complexity $\mathcal{O}\left(N_{\mathrm{RF}}Q\Omega\right)$. Finally, in step 14, the LS algorithm is used again like steps 8 and 11, where $\bar{\mathbf{W}}\left(:,\tilde{\mathcal{T}}_m\right)$ is of size $QN_{\mathrm{RF}} \times \mathrm{Card}\left(\tilde{\mathcal{T}}_m\right)$ and $\bar{\mathbf{y}}_m$ is of size $QN_{\mathrm{RF}} \times 1$. As a result, this step has the complexity $\mathcal{O}\left(N_{\mathrm{RF}}Q\mathrm{Card}^2\left(\tilde{\mathcal{T}}_m\right)\right)$, where $\mathrm{Card}\left(\tilde{\mathcal{T}}_m\right) \leq L\left(2\Omega+1\right)$.

Based on the discussion above, the overall complexity of the proposed SSD-based scheme can be summarized by

$$\mathcal{O}\left(NML\right) + \mathcal{O}\left(MN_{\mathrm{RF}}QIL\Omega^2\right) + \mathcal{O}\left(MN_{\mathrm{RF}}QL^2\Omega^2\right). \tag{20}$$

By contrast, the complexity of both the OMP-based and SOMP-based schemes can be presented by $\mathcal{O}\left(MN_{\mathrm{RF}}QL^3\Omega^3\right) + \mathcal{O}\left(NMN_{\mathrm{RF}}QL\Omega\right)$ [8], [9]. Note that a small I (e.g., $I = 2$) is usually enough to guarantee the performance as will be verified later, we can conclude that the complexity of the proposed SSD-based scheme is lower than the conventional OMP-based and SOMP-based schemes.

IV. Simulation Results

In this section, we consider a wideband multiuser mmWave MIMO-OFDM system, where the BS equips $N = 256$-element lens antenna array, $N_{\mathrm{RF}} = 8$ RF chains to serve $K = 8$ single-antenna users. The carrier frequency is $f_c = 28$ GHz, the number of sub-carriers is $M = 128$, and the bandwidth is $f_s = 4$ GHz. The spatial channel of each user in (1) is generated as follows [8]: 1) $L = 3$; 2) $\beta_l \sim \mathcal{CN}\left(0,1\right)$; 3) $\theta_l \sim \mathcal{U}\left(-\pi/2, \pi/2\right)$; 4) $\tau_l \sim \mathcal{U}\left(0, 20\mathrm{ns}\right)$ and $\max_l \tau_l = 20\mathrm{ns}$. Finally, we define the SNR for channel estimation as $1/\sigma^2$.

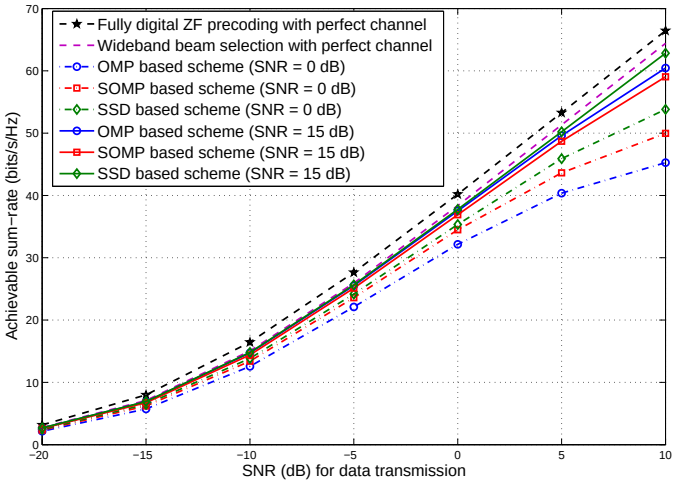

Fig. 4. Sum-rate comparison against the SNR for data transmission.

Fig. 3 shows the normalized mean square error (NMSE) performance comparison against the SNR for channel estimation, where we use $Q = 16$ instants per user for pilot transmission. For SSD based scheme, we set $\Omega = 4$ [7]. For both OMP based [9] and SOMP based [8] schemes, we assume that the sparsity level is $L(2\Omega + 1) = 27 < N_{\mathrm{RF}}Q = 128$. We also consider the oracle LS scheme as the benchmark, where the supports of wideband beamspace channel at different subcarriers are perfectly known. We observe from Fig. 3 that a small I (e.g., $I = 2$) is enough to guarantee the satisfying performance. Fig. 3 also verifies that the proposed SSD based scheme enjoys higher accuracy than OMP and SOMP based schemes in all considered SNR regions, since it can exploit the sparse structure of wideband beamspace channel. Actually, the proposed SSD based scheme has already achieved the NMSE performance very close to the oracle LS scheme.

Fig. 4 shows the achievable sum-rate of the wideband beam selection proposed in [10] with different beamspace channel estimation schemes, where $Q = 16$ and $I = 2$. We observe from Fig. 4 that by utilizing the proposed SSD based scheme instead of the conventional schemes, beam selection can achieve higher sum-rate performance, especially when the SNR for channel estimation is low (e.g., 0 dB). Moreover, Fig. 4 also shows that when SNR for channel estimation is moderate (eg., 15 dB), the wideband beam selection with the SSD based scheme can already achieve the sum-rate performance not far away from the one with perfect channel.

V. Conclusions

In this paper, we proposed an efficient SSD based beamspace channel estimation scheme for wideband mmWave MIMO with lens antenna array. We first proved that each path component of the wideband beamspace channel enjoys a unique frequency-varying sparse structure. Based on this, we then proposed to estimate the path support of each path component one by one until all path components have been considered. The complexity analysis showed that our scheme enjoys low complexity. Simulation results verified that our scheme achieves better performance than existing schemes in all considered SNR regions. For future work, we will extend the proposed scheme to 3D systems, where the elevation directions are also considered.

Acknowledgments

This work was supported by National Natural Science Foundation of China for Outstanding Young Scholars (Grant No. 61722109), Royal Academy of Engineering through the UK-China Industry Academia Partnership Programme Scheme (Grant No. UK-CIAPP\49), and US National Science Foundation (Grant Nos. 1629713, 1703389, and 1548996).

References

[1] X. Gao, L. Dai, and A. M. Sayeed, "Low RF-complexity technologies to enable millimeter-wave MIMO with large antenna array for 5G wireless communications," to appear in *IEEE Commun. Mag.*, 2018.

[2] X. Gao, L. Dai, S. Han, C.-L. I, and R. W. Heath, "Energy-efficient hybrid analog and digital precoding for mmWave MIMO systems with large antenna arrays," *IEEE J. Sel. Areas Commun.*, vol. 34, no. 4, pp. 998–1009, Apr. 2016.

[3] Y. Zeng, R. Zhang, and Z. N. Chen, "Electromagnetic lens-focusing antenna enabled massive MIMO: Performance improvement and cost reduction," *IEEE J. Sel. Areas Commun.*, vol. 32, no. 6, pp. 1194–1206, Jun. 2014.

[4] A. M. Sayeed and J. Brady, "Beamspace MIMO for high-dimensional multiuser communication at millimeter-wave frequencies," in *Proc. IEEE GLOBECOM*, Dec. 2013, pp. 3679–3684.

[5] A. Alkhateeb, O. El Ayach, G. Leus, and R. W. Heath, "Channel estimation and hybrid precoding for millimeter wave cellular systems," *IEEE J. Sel. Top. Signal Process.*, vol. 8, no. 5, pp. 831–846, Oct. 2014.

[6] J. Hogan and A. M. Sayeed, "Beam selection for performance-complexity optimization in high-dimension MIMO systems," in *Proc. CISS*, Mar. 2016, pp. 337–342.

[7] X. Gao, L. Dai, S. Han, I. Chih-Lin, and X. Wang, "Reliable beamspace channel estimation for millimeter-wave massive MIMO systems with lens antenna array," *IEEE Trans. Wireless Commun.*, vol. 16, no. 9, pp. 6010–6021, Sep. 2017.

[8] Z. Gao, C. Hu, L. Dai, and Z. Wang, "Channel estimation for millimeter-wave massive MIMO with hybrid precoding over frequency-selective fading channels," *IEEE Commun. Lett.*, vol. 20, no. 6, pp. 1259–1262, Jun. 2016.

[9] K. Venugopal, A. Alkhateeb, N. G. Prelcic, and R. W. Heath, "Channel estimation for hybrid architecture based wideband millimeter wave systems," *IEEE J. Sel. Areas Commun.*, vol. 35, no. 9, pp. 1996–2009, Sep. 2017.

[10] J. Brady and A. M. Sayeed, "Wideband communication with high-dimensional arrays: New results and transceiver architectures," in *Proc. IEEE ICC Workshops*, Jun. 2015, pp. 1042–1047.

[11] F. Rusek, D. Persson, B. K. Lau, E. G. Larsson, T. L. Marzetta, O. Edfors, and F. Tufvesson, "Scaling up MIMO: Opportunities and challenges with very large arrays," *IEEE Signal Process. Mag.*, vol. 30, no. 1, pp. 40–60, Jan. 2013.

[12] R. W. Heath, N. Gonzalez-Prelcic, S. Rangan, W. Roh, and A. M. Sayeed, "An overview of signal processing techniques for millimeter wave MIMO systems," *IEEE J. Sel. Top. Signal Process.*, vol. 10, no. 3, pp. 436–453, Apr. 2016.

[13] T. S. Rappaport, S. Sun, R. Mayzus, H. Zhao, Y. Azar, K. Wang, G. N. Wong, J. K. Schulz, M. Samimi, and F. Gutierrez, "Millimeter wave mobile communications for 5G cellular: It will work!" *IEEE Access*, vol. 1, pp. 335–349, May 2013.

[14] D. Tse and P. Viswanath, *Fundamentals of wireless communication*. Cambridge university press, 2005.

[15] W. U. Bajwa, J. Haupt, A. M. Sayeed, and R. Nowak, "Compressed channel sensing: A new approach to estimating sparse multipath channels," *Proc. IEEE*, vol. 98, no. 6, pp. 1058–1076, Jun. 2010.

[16] R. Méndez-Rial, C. Rusu, N. González-Prelcic, A. Alkhateeb, and R. W. Heath, "Hybrid MIMO architectures for millimeter wave communications: Phase shifters or switches?" *IEEE Access*, vol. 4, pp. 247–267, Jan. 2016.